Aggregate

WILEY

Aggregate Open Access

RESEARCH ARTICLE OPEN ACCESS

Ultrafast Excitonic Transitions in Enantiopure and Racemic Squaraine Thin Films

Robin Bernhardt[1] | Lukas Rieland[1] | Tianyi Wang[1] | Marvin F. Schumacher[2] | Arne Lützen[2] | Manuela Schiek[3] | Paul H. M. van Loosdrecht[1]

[1]Institute of Physics II, University of Cologne, Cologne, Germany | [2]Kekulé-Institute for Organic Chemistry and Biochemistry, University of Bonn, Bonn, Germany | [3]Center for Surface- and Nanoanalytics (ZONA), Institute for Physical Chemistry (IPC) & Linz Institute for Organic Solar Cells (LIOS), Johannes Kepler University, Linz, Austria

Correspondence: Robin Bernhardt (bernhardt@ph2.uni-koeln.de) | Tianyi Wang (twang@ph2.uni-koeln.de) | Manuela Schiek (manuela.schiek@jku.at) | Paul H. M. van Loosdrecht (pvl@ph2.uni-koeln.de)

Received: 20 August 2024 | **Revised:** 24 September 2024 | **Accepted:** 16 October 2024

Funding: This study was supported by the Deutsche Forschungsgemeinschaft (DFG, RTG-2591, and Template-designed Organic Electronics-TIDE), and Linz Institute of Technology (LIT-2019-7-INC-313 SEAMBIOF, LI1013770001- 2D3M).

Keywords: chirality | excitons | molecular aggregation | transient absorption | ultrafast dynamics

ABSTRACT

While chirality is a prevalent character of numerous biological and synthetic organic molecules, its selective absorption of circularly polarized light, known as circular dichroism (CD), is typically small due to intrinsically weak coupling between magnetic and electric dipoles. However, thin films of aggregated, enantiopure prolinol-derived squaraine molecules (ProSQ-C16) exhibit an unusually large excitonic CD signal, although the underlying mechanism is not yet known. In this study, we employ steady-state and ultrafast transient absorption spectroscopy to investigate the nature and dynamics of excitons in aggregates of enantiopure and racemic ProSQ-C16 thin films. Highly resembling transient responses of enantiopure thin films under excitations at different photon energies strongly indicate that a single type of aggregate dominates the linear optical response, that is, a strong red-shifted (J-like) and weak blue-shifted (H-like) absorption band. On the other hand, the transient properties of the racemic thin film deviate from this pattern and remain largely ambiguous. The short lifetime of excited states and coherent oscillations present in the dynamics of the transient absorption signal indicate that the early time dynamics are governed by a transition towards a dark intermediate state, which might arise from intermolecular charge transfer with potential contributions from the coupling of excitons to the vibrations. This non-radiative relaxation pathway explains the unusually weak fluorescence of the predominately J-like behaving aggregate. Our findings conclusively show that the chiral aggregate structure has a strong impact on the optical and dynamic response of the excitons and underline the significance of non-Frenkel exciton states for the optical properties of anilino squaraine dyes.

1 | Introduction

The photophysical properties of aggregated natural and synthetic molecular dyes in many cases are governed by their excitonic states [1, 2]. These excitonic states are a result of intermolecular interactions [3], which are controlled by the packing of the chromophores in an aggregate. Traditional molecular exciton theory [3] covers Coulombic interactions (Frenkel excitons) and the formation of archetypical H- and J-aggregates as well as "oblique" aggregates (Davydov splitting [4]). However, both vibronic coupling and intermolecular charge transfer can significantly impact the photophysical properties [5]. Aggregates

This is an open access article under the terms of the Creative Commons Attribution License, which permits use, distribution and reproduction in any medium, provided the original work is properly cited.

© 2024 The Author(s). *Aggregate* published by SCUT, AIEI, and John Wiley & Sons Australia, Ltd.

of quadrupolar anilino squaraine dyes exhibit distinct excitonic absorption signatures within the visible to deep-red spectral range [6]. These exciton states depend on the spatial alignment of the π-conjugated molecular backbones, which can be facilitated by non-chromophoric terminal functionalization patterns [7]. They can be predominately of Frenkel-excitonic nature [8–12] or are hybridized with intermolecular charge transfer states [11, 13, 14] and exhibit excitonic CD upon chiral functionalization [7, 15–19].

Chirality is a symmetry property primarily referring to the structural non-superimposability of an object with its mirror image, which can give rise to optical activity (circular birefringence (CB) and circular dichroism (CD)), as well as circularly polarized light emission and spin polarization effects (e.g., chirality-induced spin selectivity (CISS)) [20, 21]. For natural chiral molecular and supramolecular systems, CD is typically a weak effect because it arises from coupling of magnetic and electric dipoles, which is inherently weak in molecular materials [22, 23]. The chiroptical response of engineered materials such as liquid crystals [24], periodic nanostructures [25] and chiral metamaterials [26] is spectroscopically almost indistinguishable from intrinsic CD, even though it emerges from a different physical origin, as it is based on spatial dispersion rather than interactions of magnetic and electric dipoles [25]. Structural CD is often several orders of magnitude larger than intrinsic CD. Nevertheless, the development of strongly intrinsically CD-active organic semiconductors for chiroptical applications is an undauntedly active field of research [27–31].

In this context, a group of prolinol-derived anilino squaraines (ProSQs) were developed, demonstrating a giant intrinsic excitonic CD in dispersed aggregates and thin films [32, 33]. In particular, annealed thin films of enantiopure ProSQ carrying a sixteen carbon atom long terminal alkyl chain (ProSQ-C16) showed an optical dissymmetry factor of ± 0.75—by far the highest value for small molecule assemblies [33]. Moreover, the linear absorbance of enantiopure ProSQ-C16 thin films is beyond archetypical H- and J-aggregation. While a strong J-like redshift of the main absorption band compared to the monomer is observed for this thin film, the fluorescence is surprisingly weak. Furthermore, the line shape of this main absorption band is not symmetric, and a low-amplitude absorbing continuum extending to the weaker blue-shifted absorption band is observed. These optical and excitonic properties of aggregated enantiopure ProSQ-C16 thin films can further be tuned by interaction with a gold substrate layer, leading to exciton-plasmon coupling which strongly enhances delocalization of the excitons [34]. Due to the lack of a conclusive structural model, the underlying structure-property relationship responsible for these optical properties has not been resolved so far. Two different scenarios have been proposed via theoretical modeling for dispersed aggregates involving either intermolecular charge transfer or a network of coexisting aggregates [32], which asks for more experimental evidence.

In this study, we conduct ultrafast transient absorption spectroscopy on enantiopure and racemic thin films of ProSQ-C16 on glass substrates to provide a deeper insight into the excitonic properties and the structural nature of their aggregation. Using transient absorption spectroscopy we confirm a J-aggregate-like character of the main absorption band and the connection of the J- and H-like absorption bands via a common ground state, indicating a single type of aggregate for both enantiopure thin films. It has already been shown that intermolecular charge transfer must be accounted for if the absorption pattern originates from a single aggregate [32].

The transient absorption dynamics reveal that inside this aggregate, an efficient non-radiative decay channel exists that converts the first excited singlet state into an optically dark intermediate state. This transition might explain the lack of fluorescence, potentially due to a conical intersection between the initially excited and an intermediate dark state, as is hinted by the coherent oscillations observed in the early transient dynamics. As expected, the racemic thin film does not exhibit excitonic CD, but the linear and transient absorption properties are also influenced by the heterogeneity of the aggregation. Our study highlights the importance of linear and transient excitonic properties in understanding the structure-property relationship of these extraordinary chiral molecular aggregates, as well as the significance of charge transfer interactions for the linear, chiral and transient optical properties.

2 | Results

2.1 | Steady-State Absorption

The molecular structure of one of the enantiopure ProSQ-C16, (*S,S*)-ProSQ-C16, is shown in Figure 1a. Thermal annealing of the spincasted enantiopure and racemic ProSQ-C16 thin films ensures molecular aggregation, which leads to absorbance spectra as shown in Figure 1b. The enantiopure thin films exhibit the already-known spectral signatures of a single asymmetric and strong red-shifted transition (J-band) centered around 1.6 eV (about 780 nm) and a weaker blue-shifted transition (H-band) at 2.2 eV (about 550 nm) with respect to the absorbance spectrum of the monomer [33, 34]. While the shapes and spectral positions of the main features are the same in both enantiopure thin films, differences between the enantiopure and racemic films become evident. The racemic film absorbs with two closely spaced sub-bands at 1.615 eV and 1.675 eV, which both are blue-shifted with respect to the much sharper absorption band in the enantiopure films. In addition, the weaker H-band has almost disappeared in the racemic film. Instead, a long absorptive tail emerges, extending from the two J-bands to higher energies. These clearly visible differences in the absorbance spectra are the first indications of a different aggregate packing in the racemic thin film with respect to the enantiopure films. The intermolecular arrangement must be significantly altered on the nanometer scale, which makes the existence of discrete chiral domains of (*R,R*) and (*S,S*) moieties in the racemic film unlikely.

The overall interaction with light is remarkably high, as quantified by the (effective) uniaxial complex refractive indices for the chiral and racemic thin films shown in Figures S1a and S1c, respectively. The maxima of the ordinary extinction coefficients of the J-band range from 3.0 for the chiral thin films to 2.0 for the racemic thin films. Although the value for the racemic thin film is significantly lower compared to the chiral thin films, it still by far exceeds the typical range for conjugated polymer thin films, which often appears to be limited to 1.0 [35]. From the uniaxial anisotropy of both the enantiopure and racemic

26924560, 2025, 3, Downloaded from https://onlinelibrary.wiley.com/doi/10.1002/agt2.698 by Bibl. der Universitat zu Koln, Wiley Online Library on [12/11/2026]. See the Terms and Conditions (https://onlinelibrary.wiley.com/terms-and-conditions) on Wiley Online Library for rules of use; OA articles are governed by the applicable Creative Commons License

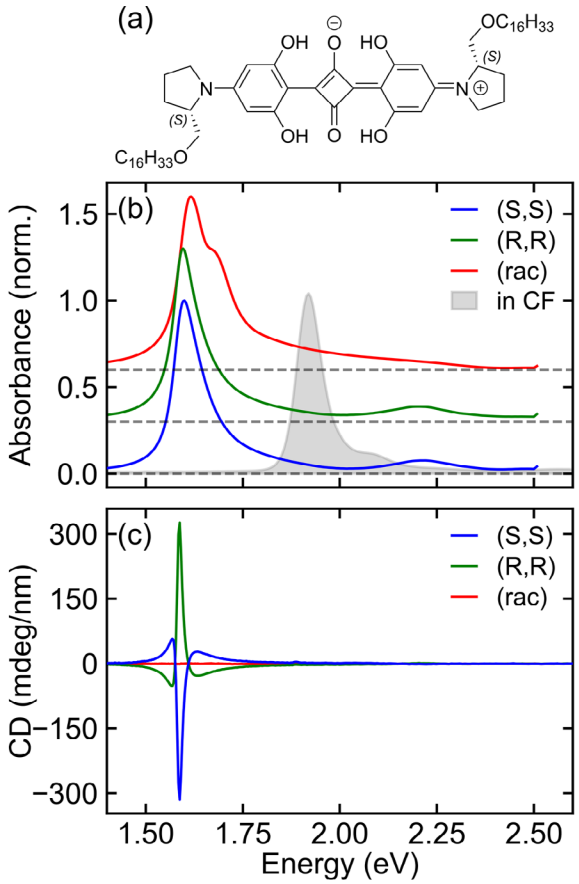


FIGURE 1 | (a) Molecular structure of (*S,S*)-ProSQ-C16 with the stereogenic C atom marked with "*(S)*". (b) Normalized steady-state absorbance spectra of the ProSQ-C16 thin films examined in this study, as well as monomeric (*S,S*)-ProSQ-C16 in a chloroform (CF) solution as reference (grey spectrum). (*S,S*)/(*R,R*) denotes the enantiopure thin film only containing (*S,S*)- or (*R,R*)-ProSQ-C16, and (rac) the racemic thin film. The absorbance baseline is offset by 0.3 and 0.6 for the (*R,R*) and (*rac*) thin film, respectively. (c) Thickness normalized circular dichroism (CD) spectra extracted from the matrix logarithm of reconstructed normal incidence transmission Mueller matrix measurements of spincasted and annealed thin films of (*R,R*)- and (*S,S*)-ProSQ-C16 as well as (*rac*)-ProSQ-C16.

thin films, it is evident that the H-like transition is basically oriented perpendicular to the plane of the thin films (extraordinary components of the complex refractive index). Therefore, this H-band appears only weakly in all normal incidence steady-state and transient transmission measurements discussed in this study, while the J-like transition is mainly oriented within the plane of the thin films (ordinary components of the complex refractive index) and dominates the spectra.

Circular dichroism (CD) spectra of the enantiopure and the racemic thin films are shown in Figure 1c. The enantiopure thin films feature sharp conservative excitonic CD signals of opposite sign, peaking at about 1.6 eV. Thus, almost all of the CD rotational strength has relocated to the J-band transition. This CD signal scales linearly with layer thickness (see Figure S1b), as expected for an intrinsic excitonic circular dichroism [33]. From this it can be inferred that aggregate morphology and dimensions are consistent for the enantiopure thin film samples under investigation. In contrast, the racemic layer shows no CD regardless of the layer

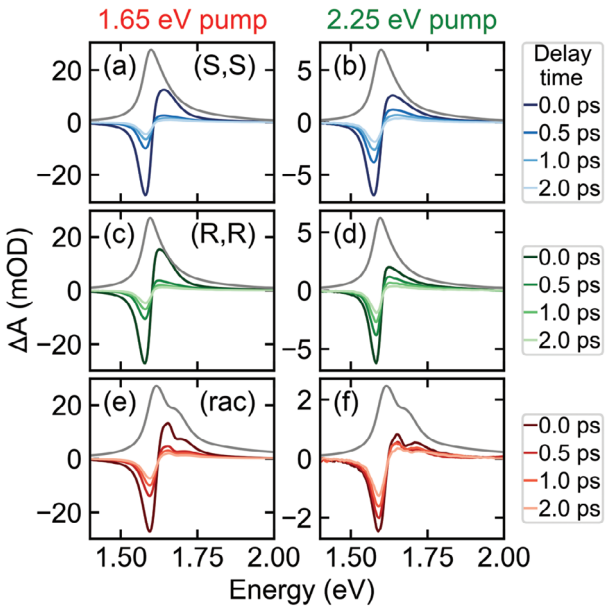


FIGURE 2 | Transient absorption spectra upon photoexcitation at 1.65 eV (750 nm) (a,c,e) and at 2.25 eV (550 nm) (b,d,f) for selected delay times as indicated in the legend for a fluence of 400 W/cm^2. Blue colors show the transient absorption spectra of (*S,S*)-ProSQ-C16 thin film (a,b), green colors the (*R,R*)-ProSQ-C16 thin film (c,d), and red colors the racemic film (e,f). The grey line shows the steady-state absorbance spectrum of the given sample for reference in arbitrary units.

thickness (see also Figure S1d). Since the steady-state absorbance spectrum of the racemic thin film differs significantly from that of the enantiopure films, it seems unlikely that enantiopure aggregate domains with opposite chirality would be formed [36]. Even if there were discrete S-S and R-R interactions that cause resolution of the racemic mixture into chiral subdomains, they would be of equal number. As long as the CD measurement is an integral method like in this case, racemic samples will always be CD-silent.

2.2 | Transient Absorption

To investigate the nature of excitons within the thin film more thoroughly, transient absorption measurements are carried out by selectively exciting either the J-band or the H-band of each thin film. The spectral transient response of the respective thin films, (*S,S*), (*R,R*), (*rac*), can be seen in Figure 2a,c,e for J-band excitation and Figure 2b,d,f for H-band excitation, along with the steady-state absorbance of the corresponding thin films. In all measurements, the amplitude of the transient response is outstandingly high, further emphasizing the extremely strong light-matter interaction in ProSQ-C16 aggregates [12, 37, 38].

The transient response of the enantiopure films to J-band excitation (Figure 2a,b) is dominated by strong negative bleach signal around the J-band, coupled to blue-shifted photo-induced absorption (PIA) signals, as observed before [34]. This is in line with the well-established footprint of J-aggregates [39], where the negative bleach signal carries both ground-state bleach (GSB) and stimulated emission (SE) contributions. It is important to note that the spectral shape of each sample does not depend on the fluence of the photoexcitation. The amplitude of the initial

26924560, 2025, 3, Downloaded from https://onlinelibrary.wiley.com/doi/10.1002/agt2.698 by Bibl. der Universitat zu Koln, Wiley Online Library on [12/11/2026]. See the Terms and Conditions (https://onlinelibrary.wiley.com/terms-and-conditions) on Wiley Online Library for rules of use; OA articles are governed by the applicable Creative Commons License

transient response remains proportional to the fluence even at very high excitation densities (see Figure S2).

The shapes of the transient absorption spectra of the two enantiopure thin films are highly similar, with the only difference being the slightly sharper low-energy shoulder of the PIA signal in the (*R,R*)-ProSQ-C16 thin film. The residual difference in the spectra could be due to a minimal difference in enantiomeric purity and the experimental uncertainty in the thin film preparation [33], which could lead to a different extent of aggregation and disorder in the films. The film thickness of the (*R,R*) and (*S,S*) samples is approximately 28 nm and 22 nm, respectively, and is thus a variable parameter related to processing.

Compared to direct excitation of the J-band at 1.65 eV, photoexcitation at the H-band at 2.25 eV reveals an almost identical transient response around the J-band for both enantiopure films, with an amplitude consistent with the weaker absorbance of the H-band compared to the J-band. This strong resemblance suggests that the initially excited exciton state corresponding to the H-band rapidly relaxes into the excitonic state corresponding to the J-band. This strongly suggests that the two absorption lines of the enantiopure thin films originate from the same type of aggregate and share the same ground state.

In contrast, the transient response of the racemic thin film is more complicated. While both the bleach and PIA signals can be identified as for the enantiopure thin films, a substructure between 1.65 eV and 1.8 eV arises in the PIA signal. At least two peaks can be recognized in the PIA signal, whose peak energies correspond to one of the optical bright states seen in the steady-state absorbance spectrum. A proper assignment of these peaks is difficult, as bleach signals and PIA signals from different excitonic states might overlap.

Exciting the weakly absorbing H-band of the racemic thin film results in distinct changes to the transient spectra compared to direct excitation of the J-bands. The relative amplitude of the PIA features is significantly reduced when the H-band is excited, and the spectral shape of the PIA sub-peaks does not match the transient response of J-band excitation either. The bleach signal, on the other hand, appears to be consistent in both sets of measurements. This implies to some extent an efficient transition from the H-band to the J-bands, while the exact distribution of populated excitonic states differs between the 1.65 eV and 2.25 eV photoexcitation conditions. In contrast to the enantiopure thin films, the transient response of the racemic thin film cannot be unambiguously assigned as J-aggregate-like. The thermal annealing process does not seem to cause resolution of the racemic mixture into an equivalent number of enantiopure aggregate domains. Instead, multiple types of equally stable racemic aggregates are most likely formed [36].

2.3 | Transient Absorption Dynamics

Further insights into the excitonic nature of the enantiopure and racemic ProSQ-C16 aggregates are revealed by the dynamics of individual bleach and PIA signals and their fluence dependence, as is shown in Figure 3. Overall, the dynamics in all thin films are rather fast when compared to other SQ aggregates [8, 12, 15]. Within this fast response window (<4 ps), the bleach and PIA signals show different dynamics across all measurements.

All PIA signals decay faster than their bleach counterparts under the same measurement condition. This holds true for all samples, fluences and photoexcitation energies, and can be seen most clearly by the different remaining signals at a delay time of 4 ps in Figure 3. In the context of two exciton absorption [39], the PIA and SE signals persist as long as the exciton band minimum (J-band) is occupied, while the ground-state bleach persists until the ground-state is occupied again. The mismatch between PIA and bleach dynamics therefore requires an intermediate state, into which excitons can transition.

As expected, the dynamics of two enantiopure thin films are almost identical to each other, which again demonstrates that they adopt the same (mirror-imaged) aggregate structure. On the contrary, the racemic thin film shows much slower dynamics at lower fluences, which are accelerating significantly with increasing fluence. Even though all thin films exhibit fluence-dependent dynamics, it is much more pronounced in the racemic sample.

Further insights can be gained by fitting of the bleach dynamics of the racemic thin film with multi-exponential decay functions (see Section S3 for all fit functions used and Tables S1–S6 and Figure S3 for the fit results of all samples). The fitting results suggest multiple dynamic contributions with different decay times. The apparent acceleration of the dynamics for higher fluences seems to be caused by an increase in the relative amount of excitons undergoing fast decay at the expense of the slower decay channels. A consistent trend is observable only for the racemic thin film, but not for the enantiopure films, which might indicate different relaxation mechanisms.

Additionally to the decay observed for the PIA and bleach dynamics, coherent oscillations can be found in the spectral region between PIA and bleach signals. These coherent oscillations are visible for all thin films, but only when the J-band is directly excited at 1.65 eV. After careful subtraction of the exponentially decaying population signal using a fitted single exponential decay function, the clearly visible coherent oscillations are presented in Figure 4a,c,e, for all three samples. The Fourier-transform of the residuals (Figure 4b,d,f) shows that the oscillations occur at a frequency of 4.3 THz or approximately 144 cm^{-1}, which applies to all films and suggests a molecular origin. Similar coherent oscillations at 147 cm^{-1} were found in monomeric ProSQ-C16 in solution also on ps-timescale, and were identified as a collective molecular backbone vibration [40] of a single molecule of ProSQ-C16. The fact that this mode is observed in both enantiopure and racemic thin films further suggests that this vibrational mode is insensitive to the aggregate structure, and is intrinsic to a single molecule. The lack of coherent oscillations under H-band excitation can be caused by incoherent relaxation of the excitons from the H-band to the J-band—therefore coherence is lost before the J-band excitons can couple to vibrational degrees of freedom.

2.4 | Singular Value Decomposition

In order to disentangle different correlated spectral and dynamical contributions, singular value decomposition (SVD) is

26924560, 2025, 3, Downloaded from https://onlinelibrary.wiley.com/doi/10.1002/agt2.698 by Bibl. der Universitat zu Koln, Wiley Online Library on [12/11/2026]. See the Terms and Conditions (https://onlinelibrary.wiley.com/terms-and-conditions) on Wiley Online Library for rules of use; OA articles are governed by the applicable Creative Commons License

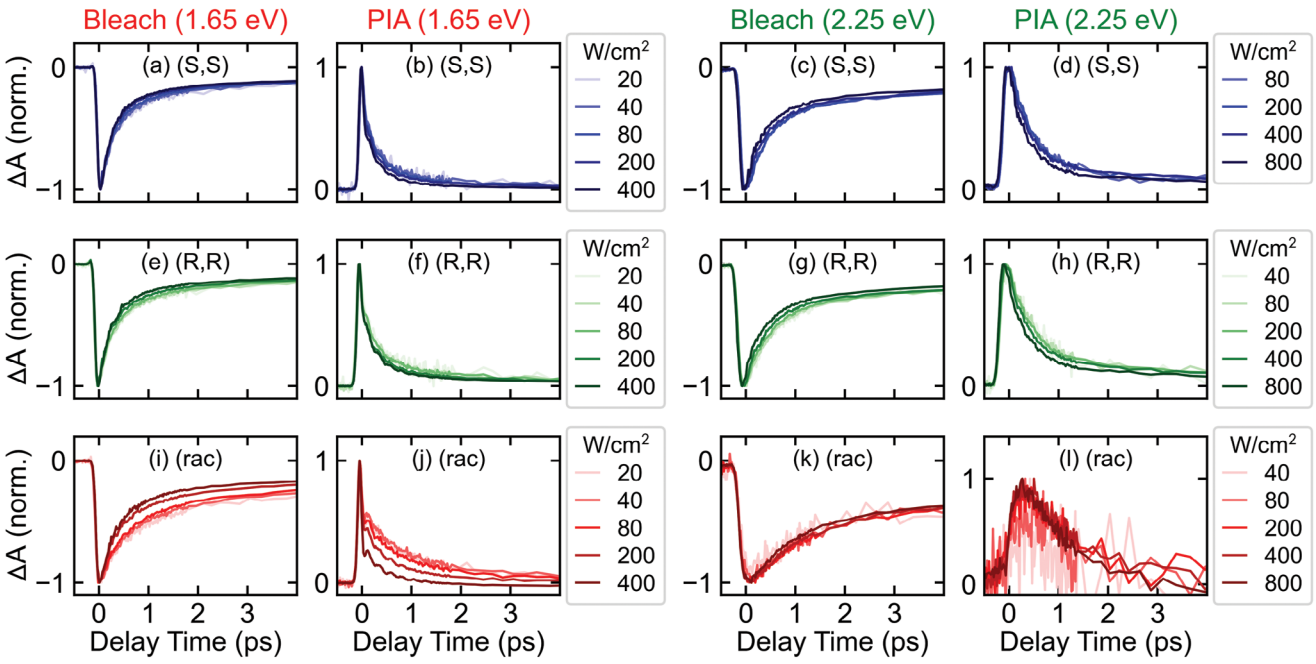


FIGURE 3 | Fluence-dependent dynamics of bleach (a,c,e,g,i,k) and photoinduced absorption (b,d,f,h,j,l) signals. Data from (*S,S*) enantiopure thin films are shown in blue, (*R,R*) in green, and racemic in red. Left side spectra represent a photoexcitation at 1.65 eV (750 nm), right side 2.25 eV (550 nm) photoexcitation.

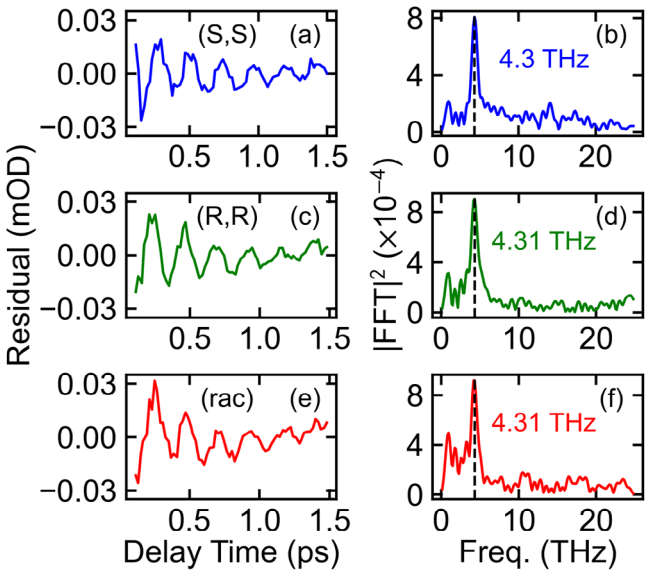


FIGURE 4 | Coherent oscillations in the residual of an exponential fit to the transient dynamics at 1.65 eV (a,c,e) and the corresponding Fourier-transform frequency spectra (b,d,f). The dynamics were obtained at the photon energy showing the most pronounced oscillations ((*S,S*): 1.625 eV; (*R,R*): 1.616 eV; (*rac*): 1.636 eV).

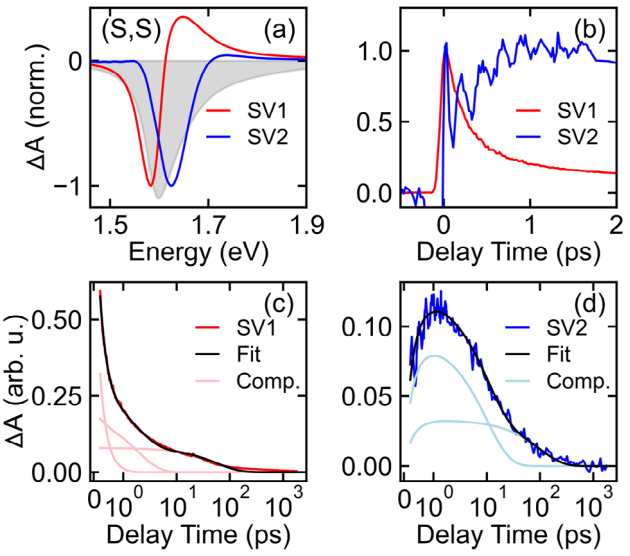


FIGURE 5 | Spectra and dynamics of the two relevant singular values obtained from the transient absorption data of the (*S,S*)-ProSQ-C16 thin film excited at 1.65 eV with a fluence of 400 W/cm². (a) Spectra of the first two singular values (SV), both demonstrating shifts of the negative features with respect to the inverted absorption maximum indicated by the gray shading. (b) Time traces associated with the singular values. (c) Fit of the dynamics of the first singular value dynamics using three exponential decay components, each shown. (d) Fit of the second singular value dynamics, with a function containing two initially rising and decaying components.

performed for a series of high fluence measurements, yielding characteristic time-independent singular value spectra as well as wavelength-independent singular value dynamics of different transient processes [41]. The results for the (*S,S*)-ProSQ-C16 thin film is shown in Figure 5, the corresponding results for the (*R,R*)- and (*rac*)-ProSQ-C16 thin films can be found in Figure S4 in Section S4.

For datasets obtained with J-band excitation, the first two singular values have a large impact on the transient absorption data. For datasets obtained with H-band excitation, the singular value decomposition did not yield constructive results, neither for the

26924560, 2025, 3, Downloaded from https://onlinelibrary.wiley.com/doi/10.1002/agt2.698 by Bibl. der Universitat zu Koln, Wiley Online Library on [12/11/2026]. See the Terms and Conditions (https://onlinelibrary.wiley.com/terms-and-conditions) on Wiley Online Library for rules of use; OA articles are governed by the applicable Creative Commons License

TABLE 1 | Fitting results of singular value dynamics of the transient absorption spectrum of (*S,S*)-ProSQ-C16.

Data	A_1	t_1 (ps)	A_2	t_2 (ps)	A_3	t_3 (ps)
SV1	0.342 ± 0.007	0.242 ± 0.009	0.176 ± 0.007	1.75 ± 0.12	0.0796 ± 0.0024	57.1 ± 3.5
SV2	0.133 ± 0.004	0.364 ± 0.021	0.524 ± 0.095	0.452 ± 0.046	—	50.2 ± 7.2

racemic nor the enantiopure films, and therefore will not be discussed. For the enantiopure films, the spectral shape is consistent (Figures 5a and S4a): the first singular value largely resembles the J-aggregate-like transient absorption spectra after relatively short delay times and shows both bleach and photoinduced absorption signals. Its spectral shape is in line with the spectral signature of J-band occupation. The spectral response of the second singular value is dominated by a bleach signal, which has a similar spectral shape to the J-band absorption maximum but is blue-shifted, alongside a minuscule photoinduced absorption signal. This spectrum on the other hand might belong to the population of the intermediate state. The apparent spectral shift of the ground state bleach might be simply related to the absence of stimulated emission, which is commonly red-shifted with respect to the ground state bleach signal. Alternatively, a spectral shift of the absorbance line due to the population of other states or even a non-negligible transient reflectance contribution might be responsible for the spectral discrepancy [42, 43].

Similar to the spectral components, singular value dynamics differ significantly from each other (Figures 5b and S4b). Note that the strong negative feature of the second singular value dynamics is a decomposition artifact due to dynamical dispersion. While the dynamics of the first singular value are of purely decaying nature, a distinct growth can be seen for the second singular value. Additionally, the first singular value dynamics show a smooth decay, while the second dynamics clearly contain oscillations that echo the coherent oscillations observed in the dynamics of certain regions of the TA spectra. The spectral position of the coherent oscillations and the second singular value demonstrate a high degree of overlap.

To quantify the dynamics of the singular values and their relationship to each other, we fitted the dynamics considering two different fit functions. For the first singular value, at least three exponential decays are needed to fit the dynamics

$$f_1(t) = A_1 \cdot e^{\frac{-t}{\tau_1}} + A_2 \cdot e^{\frac{-t}{\tau_2}} + A_3 \cdot e^{\frac{-t}{\tau_3}}, \quad (1)$$

while for the second, the growing and decaying dynamics required a fit function with at least one growing component and two considered exponential decay functions

$$f_2(t) = A_1 \cdot \left(1 - e^{\frac{-t}{\tau_1}}\right)\left((1 - A_2) \cdot e^{\frac{-t}{\tau_2}} + A_2 \cdot e^{\frac{-t}{\tau_3}}\right). \quad (2)$$

The fit results are summarized in Table 1 and can be seen in Figure 5c,d for the (*S,S*)-ProSQ-C16 thin film (see Figure S4c,d,g,h and Tables S7 and S8 for the fit results of (*R,R*)- and racemic ProSQ-C16 thin films).

The multiple exponential decays of the SV1 dynamics indicate multiple relaxation channels and sub-populations of the initially excited states over a variety of time scales. While the shortest component (≈0.24 ps) makes the dominant contribution, a considerable fraction of the excited states relaxes more slowly (≈1.75 ps), while an even smaller fraction decays only after ≈57 ps. Similar to the SV1 dynamics, the decay of the SV2 dynamics requires two components after the signal rises for about 0.36 ps, with a fast ($1 - A_2$, ≈0.5 ps) and slow (A_2, ≈50 ps) decay of equal amplitude.

The time scales of both the fastest and slowest components of each SV dynamics are closely related. The rapid growth of SV2 coincides with the decay of SV1, suggesting a fast transition from one state represented by the first singular value to another associated with the second singular value. The long-time component indicates that both underlying excitonic states also possess a slowly decaying sub-population.

For the racemic thin film (see Figure S4e–h), the spectrum of SV1 resembles the initial transient absorption spectra, similar to the enantiopure thin films. On the other hand, the spectrum of SV2 deviates from a simple bleach profile, as the width of the negative feature is much narrower than the absorption line. Moreover, the side peak of the SV2 spectrum does not match the steady-state absorption spectrum, neither in relative position nor in relative amplitude. In addition to the spectral discrepancies, the SV2 dynamics of the racemic layer cannot be fitted with the fit functions applied to the enantiopure SV2 dynamics. This implies that these functions, which describe the dynamics of the enantiopure film, must be extended with more complex contributions to accurately represent the racemic thin film's behavior.

3 | Discussions

From the transient absorption spectra, the J-like character of the enantiopure thin films becomes more evident. The presence of stimulated emission and photoinduced absorption features next to the ground state bleach and their spectral shape are clear indications that the bright state observed as the J-band is indeed at the minimum of the exciton band, which is the fundamental requirement for a J-aggregate. Additionally, the appearance of a J-like transient signal after photoexcitation of the H-band represents compelling evidence for the J-band being the lowest exciton-band state.

Our data strongly support a "single-type-of-aggregate" picture for enantiopure thin films, in which only one single aggregate type is responsible for the light-matter interactions at visible-light frequencies. This is in line with the theoretical groundwork of Painelli and coworkers [32] that a single enantiopure aggregate

26924560, 2025, 3, Downloaded from https://onlinelibrary.wiley.com/doi/10.1002/agt2.698 by Bibl. der Universitat zu Koln, Wiley Online Library on [12/11/2026]. See the Terms and Conditions (https://onlinelibrary.wiley.com/terms-and-conditions) on Wiley Online Library for rules of use; OA articles are governed by the applicable Creative Commons License

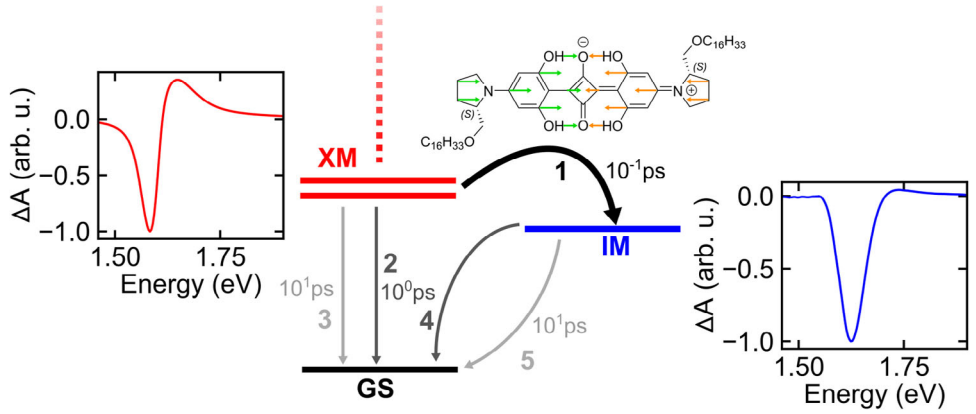


FIGURE 6 | Sketch of the exciton relaxation channels of enantiopure ProSQ-C16 aggregates. The fastest exciton dynamics are observed for a transition from the initially excited state at the low energy edge of the exciton band (XM) into the intermediate state (IM) (**1**), which might be mediated by vibronic coupling to collective molecular vibrational modes [40] (as indicated by the arrows attached to the molecular structure showing the (*S,S*)-ProSQ-C16). This migration happens extremely fast, while the transition to the ground state (GS) takes significantly longer (**4**,**5**). On longer time scales, excitons can also directly transition back into the ground state (**2**,**3**).

can lead to two absorptive peaks due to intermolecular charge transfer hybridization of excitons in dispersed colloidal ProSQ aggregates. Moreover, after some recent dispute [12], such charge-transfer Frenkel hybrid excitons were confirmed for non-chiral anilino-squaraine compounds in uniaxial and crystalline textured thin films by conclusive theoretical and experimental studies [11, 13].

Some of the observations made above partially also hold for the racemic thin film, even though the steady-state and transient spectra appear to be more convoluted. The transient response at the J-band deviates from a perfect J-aggregate-like ("J-like") response, especially for the PIA signal. Furthermore, the spectral shape and amplitude of the PIA signal depend on whether the J-band or the H-band is excited. This is a strong indication that, in contrast to the enantiopure thin films, multiple exciton bands must be responsible for the transient properties of the racemic thin film, and therefore multiple types or fractions of racemic aggregates must be present.

To understand the dynamics of all spectral features, multiple relaxation channels have to be considered, which is consistent with the dynamics obtained from SVD. We associate the first singular value signal with the occupation of the exciton band minimum (XM), and the second singular value signal with occupation of an intermediate dark state (IM), as sketched in Figure 6. The coinciding decay of the XM-related signal and growth of the IM-related signal (see Figure 5c,d) strongly suggests an excitonic transition from the XM to the IM state, which is consistent with the mismatch between the bleach and PIA dynamics. However, the XM → IM transition (**1**) cannot rationalize all facets of the dynamics, and multiple slower relaxation dynamics of both XM (**2**,**3**) and IM (**4**,**5**) have to be considered. The low fluorescence yield of the thin films suggests that the slower relaxation channels are mostly non-radiative. These dynamics might arise from recombination at traps or interfaces, or exciton-exciton annihilation processes [38, 44–49].

The nature of the reported intermediate state cannot be resolved by our study. However, considering the theoretical work done by Painelli and coworkers [32], an intermolecular charge transfer state, which is optically dark on its own [13, 14], represents a suitable candidate. Moreover, a dark state was recently experimentally evidenced by transient absorption spectroscopy in non-chiral anilino-squarain thin films, which are known to form charge-transfer Frenkel hybrid excitons [37].

The short lifetime of the excitons and their rapid transition into a dark state before relaxing back to the ground state deserves special attention. As this transition happens on the sub-ps scale, and is dressed with a strong vibronic coupling, it could possibly be mediated by a conical intersection [50, 51] that outperforms the radiative transition back to the ground state. Dynamics mediated by conical intersections have been demonstrated and hinted at for various molecular aggregates, including squaraines [19, 52, 53]. Conical intersections play an important role in biological systems as the relaxation channels act as energy scavengers to prevent photo damage [54] or they funnel efficient conversion from a reactant to a photochemical reaction product [55]. For chiral molecular systems, Berry forces occurring near a conical intersection have been predicted to enable sizable chiral-induced spin selectivity (CISS) effects [56]. While experimentally reported time scales are still sparse, both intra- and intermolecular conical intersection mediated dynamics have been reported in the timescale between 20-100 fs [50, 51, 57], which is close to the fast mechanism observed in this study. Note that the actual time scale of this process might be faster than the observed value, as the value approaches the time-resolution of the experiment.

So far, most studies on supramolecular conical intersections were focused on higher energy diatomic vibrational modes in dimer systems with highly localized states, leaving intermolecular charge transfer states largely unexplored [19, 50–53, 57–59]. In contrast, the conical intersection in the ProSQ-C16 system at hand might be characterized by a low energy vibrational mode (see Figures 4 and 6), delocalized excitonic states, and probably a large degree of intermolecular charge transfer. It will be highly valuable to further investigate these ProSQ-C16 system as well as to explore other (donor-acceptor-donor) molecular systems which could potentially help clarify the role of lower energy

26924560, 2025, 3, Downloaded from https://onlinelibrary.wiley.com/doi/10.1002/agt2.698 by Bibl. der Universitat zu Koln, Wiley Online Library on [12/11/2026]. See the Terms and Conditions (https://onlinelibrary.wiley.com/terms-and-conditions) on Wiley Online Library for rules of use; OA articles are governed by the applicable Creative Commons License

vibrations, exciton delocalization, and intermolecular charge transfer in influencing conical intersections and macroscopic properties such as circular dichroism.

4 | Conclusions

Our study employs steady-state and ultrafast transient absorption spectroscopy to investigate the nature and dynamics of excitons in enantiopure and racemic aggregates in ProSQ-C16 thin films. We observe transient spectra originating from a single type of aggregate in the enantiopure thin films of both handednesses. Our data show that the optical response of these thin films in the form of a dominant J-band and a weaker H-band originates from the hybridization of a Frenkel with a charge transfer exciton. We report a multitude of dynamical contributions, led by an efficient transition of the photoexcited exciton band within the J-aggregate of the enantiopure thin films into an optically dark intermediate state, which explains the faint fluorescence observed for these systems. We conclude that this intermediate state is of intermolecular charge transfer nature. Based on the time scales and coherent oscillations observed in the transient response of all systems, we propose that a conical intersection towards the intermediate CT state could constitute an efficient non-radiative relaxation channel. Steady-state and transient optical properties of the racemic thin film deviate significantly from a typical J-aggregate-like behavior. This highlights the added value of chirality in general and enantiopurity in particular not only for the optical activity but also for the linear and transient optical properties. Our study provides fundamental insights into the excitonic properties of a family of chiral ProSQ aggregates based on the chiral arrangement of quadrupolar anilino-squaraine backbones. These findings are key to understanding and ultimately exploiting the giant circular dichroism of a molecular system on a scale relevant for future technological applications.

5 | Materials & Methods

5.1 | Samples

The squaraine dyes (*S,S*)- and (*R,R*)-ProSQ-C16 used for thin film preparation were synthesized following literature procedures [32, 33]. As starting material, *N*-Boc-D-prolinol (Fluorochem, 99% purity) or *N*-Boc-L-prolinol (chemPUR, 99% purity) was used as received. Thus, the chiral starting materials have a comparable purity to achieve a comparable enantiomeric purity of the target compounds, which was not the case in a previous study [33]. Thin films of ProSQ-C16 were processed on pieces of float glass (25 × 25 mm^2, VWR objective slides) similar to previously established procedures [33]. Both (*S,S*)-enantiopure, (*R,R*)-enantiopure as well as racemic (one-to-one (*S,S*) and (*R,R*) mixture; (*rac*)) ProSQ-C16 solutions in amylene stabilized chloroform (concentration = 3 mg/mL) were used to produce thin films in ambient atmosphere by spincasting (1000 rpm/s acceleration to 3000 rpm kept for 60 s; 400 rpm/s acceleration to 2000 rpm kept for 60 s), followed by thermal annealing on a hotplate (surface temperature 180°C) for 30 min to ensure thermodynamically stable aggregation.

ProSQ-C16 layer thicknesses were determined by variable angle spectroscopic ellipsometry (see Section S1 for details): (*S,S*) = 22 nm (±4 nm); (*R,R*) = 28 nm (±4 nm); (*rac*) = 29 nm (±4 nm).

5.2 | Circular Dichroism

A single rotating compensator J.A. Woollam M2000-DI ellipsometer with CCD-based detection was used for a partial Mueller matrix measurement (first three rows of the Mueller matrix) at normal incidence transmission. The beam diameter is approximately 2 mm, effectively averaging over nano- and microscaled domains. Data were recorded with CompleteEASE version 5 and exported for further analysis with Matlab. The full Mueller matrix is reconstructed by an algebraic procedure before the the matrix logarithm is calculated [60]. The CD spectra are the average of the l_{14} and l_{41} elements of the differential Mueller matrix and are divided by the respective layer thickness obtained from the ellipsometric analysis (see Section S1 for further details).

5.3 | Steady-State and Transient Absorption

Both steady-state and transient absorption spectroscopy measurements were conducted using a setup based on a 150 kHz, 15 W Yb:KGW regenerative amplifier laser system (PHAROS, Light Conversion) [61]. All transmission spectra are recorded at normal incidence. For transient measurements, band-pass filtered pulses from a non-collinear optical parametric amplifier (TOPAS, Light Conversion) were used for pumping the sample with a temporal width of 100–150 fs at 1.65 eV (750 nm) and 2.25 eV (550 nm). To prevent laser-induced degradation of the aggregated films, we allowed fluences of 20 to 800 W/cm^2 and loosely focused the pump beam onto the sample with a spot size of around 160 μm in diameter. For both the probe and (quasi-)steady-state measurements, a 1450 nm pulsed laser beam was tightly focused into a 2 mm thick sapphire plate (EKSMA) to generate a white light supercontinuum. The white light beam was spectrally filtered, limiting the range to 1.37–2.48 eV (500–900 nm). Spectra were detected using a silicon-based diode array mounted in a polychromatic spectrometer (HARPIA, Light Conversion; SHAMROCK, Andor; Hamamatsu S8380-256Q with a readout circuit c7884). To minimize pump beam scattering into the detector, the polarization of the pump beam was set to be perpendicular to that of the probe, and a polarizer was placed in front of the detector to filter out most of the residual intensity of the pump beam.

Author Contributions

Robin Bernhardt and Manuela Schiek conceived the project. Robin Bernhardt, Lukas Rieland and Tianyi Wang performed the steady-state and transient optical experiments and analyzed the experimental results. Marvin F. Schumacher and Arne Lützen synthesized the squaraine molecules. Marvin F. Schumacher prepared the thin film samples. Marvin F. Schumacher and Manuela Schiek performed and analyzed the ellipsometry and polarimetry experiments. Paul H. M. van Loosdrecht

26924560, 2025, 3, Downloaded from https://onlinelibrary.wiley.com/doi/10.1002/agt2.698 by Bibl. der Universitat zu Koln, Wiley Online Library on [12/11/2026]. See the Terms and Conditions (https://onlinelibrary.wiley.com/terms-and-conditions) on Wiley Online Library for rules of use; OA articles are governed by the applicable Creative Commons License

supervised the project. Robin Bernhardt, Manuela Schiek and Tianyi Wang wrote the manuscript with contributions from all authors.

Acknowledgements

The authors gratefully acknowledge support from the Deutsche Forschungsgemeinschaft (DFG, RTG–2591 "TIDE – Template–designed Organic Electronics"). Manuela Schiek thanks the Linz Institute of Technology (LIT-2019-7-INC-313 SEAMBIOF and LI1013770001- 2D3M) for funding. Marvin F. Schumacher thanks the Manchot Foundation for a doctoral scholarship.

Conflicts of Interest

The authors declare no conflicts of interest.

Declaration of Content

This work is part of a thesis prepared toward the completion of a doctoral degree at University of Cologne and has not been published elsewhere in any peer-reviewed journals.

Data Availability Statement

The supporting data for this article are available from Zenodo via the following link: 10.5281/zenodo.14013785.

References

1. S. K. Saikin, A. Eisfeld, S. Valleau, and A. Aspuru-Guzik, "Photonics Meets Excitonics: Natural and Artificial Molecular Aggregates," *Nanophotonics* 2, no. 1 (2013): 21–38, https://doi.org/10.1515/nanoph-2012-0025.

2. A. M. Valencia, D. Bischof, S. Anhäuser, et al., "Excitons in Organic Materials: Revisiting Old Concepts With New Insights," *Electronic Structure* 5, no. 3 (2023): 033003, https://doi.org/10.1088/2516-1075/acf2d4.

3. M. Kasha, H. R. Rawls, and M. A. El-Bayoumi, "The Exciton Model in Molecular Spectroscopy," *Pure and Applied Chemistry* 11, no. 3 (1965): 371–392, https://doi.org/10.1351/pac196511030371.

4. A. S. Davydov, "The Theory of Molecular Excitons," *Soviet Physics Uspekhi* 7, no. 2 (1964): 145, https://doi.org/10.1070/PU1964v007n02ABEH003659.

5. N. J. Hestand and F. C. Spano, "Expanded Theory of H- and J-Molecular Aggregates: The Effects of Vibronic Coupling and Intermolecular Charge Transfer," *Chemical Reviews* 118, no. 15 (2018): 7069–7163, https://doi.org/10.1021/acs.chemrev.7b00581.

6. K. Ilina, W. M. MacCuaig, M. Laramie, J. N. Jeouty, L. R. McNally, and M. Henary, "Squaraine Dyes: Molecular Design for Different Applications and Remaining Challenges," *Bioconjugate Chemistry* 31, no. 2 (2020): 194–213, https://doi.org/10.1021/acs.bioconjchem.9b00482.

7. J. Zablocki, O. Arteaga, F. Balzer, et al., "Polymorphic Chiral Squaraine Crystallites in Textured Thin Films," *Chirality* 32, no. 5 (2020): 619–631, https://doi.org/10.1002/chir.23213.

8. G. de Miguel, M. Ziółek, M. Zitnan, et al., "Photophysics of H- and J-Aggregates of Indole-Based Squaraines in Solid State," *Journal of Physical Chemistry C* 116, no. 17 (2012): 9379–9389, https://doi.org/10.1021/jp210281z.

9. C. Lambert, F. Koch, S. F. Völker, et al., "Energy Transfer Between Squaraine Polymer Sections: From Helix to Zigzag and All the Way Back," *Journal of the American Chemical Society* 137, no. 24 (2015): 7851–7861, https://doi.org/10.1021/jacs.5b03644.

10. G. M. Paternò, L. Moretti, A. J. Barker, et al., "Near-Infrared Emitting Single Squaraine dye Aggregates With Large Stokes Shifts," *Journal of Materials Chemistry C* 5, no. 31 (2017): 7732–7738, https://doi.org/10.1039/C7TC01375B.

11. F. Balzer, N. J. Hestand, J. Zablocki, G. Schnakenburg, A. Lützen, and M. Schiek, "Spotlight on Charge-Transfer Excitons in Crystalline Textured n-Alkyl Anilino Squaraine Thin Films," *Journal of Physical Chemistry C* 126, no. 32 (2022): 13802–13813, https://doi.org/10.1021/acs.jpcc.2c03665.

12. R. Bernhardt, M. Manrho, J. Zablocki, et al., "Structural Disorder as the Origin of Optical Properties and Spectral Dynamics in Squaraine Nano-Aggregates," *Journal of the American Chemical Society* 144, no. 42 (2022): 19372–19381, https://doi.org/10.1021/jacs.2c07064.

13. N. J. Hestand, C. Zheng, A. R. Penmetcha, et al., "Confirmation of the Origins of Panchromatic Spectra in Squaraine Thin Films Targeted for Organic Photovoltaic Devices," *Journal of Physical Chemistry C* 119, no. 33 (2015): 18964–18974, https://doi.org/10.1021/acs.jpcc.5b05095.

14. C. A. Shen, D. Bialas, M. Hecht, V. Stepanenko, K. Sugiyasu, and F. Würthner, "Polymorphism in Squaraine Dye Aggregates by Self-Assembly Pathway Differentiation: Panchromatic Tubular Dye Nanorods versus J-Aggregate Nanosheets," *Angewandte Chemie International Edition* 133, no. 21 (2021): 12056–12065, https://doi.org/10.1002/ange.202102183.

15. H. Chen, M. S. Farahat, K. Y. Law, and D. G. Whitten, "Aggregation of Surfactant Squaraine Dyes in Aqueous Solution and Microheterogeneous Media: Correlation of Aggregation Behavior with Molecular Structure," *Journal of the American Chemical Society* 118, no. 11 (1996): 2584–2594, https://doi.org/10.1021/ja9523911.

16. A. T. Rösch, Q. Zhu, J. Robben, et al., "Helicity Control in the Aggregation of Achiral Squaraine Dyes in Solution and Thin Films," *Chemistry A European Journal* 27, no. 1 (2021): 298–306, https://doi.org/10.1002/chem.202002695.

17. J. Selby, M. Holzapfel, B. K. Lombe, et al., "Chiroptical Properties of Indolenine Squaraines With a Stereogenic Center at Close Proximity," *Journal of Organic Chemistry* 85, no. 19 (2020): 12227–12242, https://doi.org/10.1021/acs.joc.0c01422.

18. O. A. Mass, C. K. Wilson, S. K. Roy, et al., "Exciton Delocalization in Indolenine Squaraine Aggregates Templated by DNA Holliday Junction Scaffolds," *Journal of Physical Chemistry B* 124, no. 43 (2020): 9636–9647, https://doi.org/10.1021/acs.jpcb.0c06480.

19. E. Freytag, L. Kreimendahl, M. Holzapfel, et al., "Chiroptical Properties of Planar Benzobisthiazole-Bridged Squaraine Dimers," *Journal of Organic Chemistry* 88, no. 15 (2023): 10777–10788, https://doi.org/10.1021/acs.joc.3c00821.

20. J. R. Brandt, F. Salerno, and M. J. Fuchter, "The Added Value of Small-Molecule Chirality in Technological Applications," *Nature Reviews Chemistry* 1, no. 6 (2017): 1–12, https://doi.org/10.1038/s41570-017-0045.

21. B. P. Bloom, Y. Paltiel, R. Naaman, and D. H. Waldeck, "Chiral Induced Spin Selectivity," *Chemical Reviews* 4, no. 124, (2024): 1950–1991, https://doi.org/10.1021/acs.chemrev.3c00661.

22. N. S. S. Nizar, M. Sujith, K. Swathi, C. Sissa, A. Painelli, and K. G. Thomas, "Emergent Chiroptical Properties in Supramolecular and Plasmonic Assemblies," *Chemical Society Reviews* 50, no. 20 (2021): 11208–11226, https://doi.org/10.1039/D0CS01583K.

23. F. Bertocchi, C. Sissa, and A. Painelli, "Circular Dichroism of Molecular Aggregates: A Tutorial," *Chirality* 35, no. 10 (2023): 681–691, https://doi.org/10.1002/chir.23565.

24. M. Mitov, "Cholesteric Liquid Crystals With a Broad Light Reflection Band," *Advanced Materials* 24, no. 47 (2012): 6260–6276, https://doi.org/10.1002/adma.201202913.

25. B. Gompf, J. Braun, T. Weiss, H. Giessen, M. Dressel, and U. Hübner, "Periodic Nanostructures: Spatial Dispersion Mimics Chirality," *Physical Review Letters* 106, no. 18 (2011): 185501, https://doi.org/10.1103/PhysRevLett.106.185501.

26. Z. Wang, F. Cheng, T. Winsor, and Y. Liu, "Optical Chiral Metamaterials: A Review of the Fundamentals, Fabrication Methods and Applications," *Nanotechnology* 27, no. 41 (2016): 412001, https://doi.org/10.1088/0957-4484/27/41/412001.

26924560, 2025, 3, Downloaded from https://onlinelibrary.wiley.com/doi/10.1002/agt2.698 by Bibl. der Universitat zu Koln, Wiley Online Library on [12/11/2026]. See the Terms and Conditions (https://onlinelibrary.wiley.com/terms-and-conditions) on Wiley Online Library for rules of use; OA articles are governed by the applicable Creative Commons License

27. Y. Yang, R. C. de Costa, M. J. Fuchter, and A. J. Campbell, "Circularly Polarized Light Detection by a Chiral Organic Semiconductor Transistor," *Nature Photonics* 7, no. 8 (2013): 634–638, https://doi.org/10.1038/nphoton.2013.176.

28. M. Schulz, F. Balzer, D. Scheunemann, et al., "Chiral Excitonic Organic Photodiodes for Direct Detection of Circular Polarized Light," *Advanced Functional Materials* 29, no. 16 (2019): 1900684, https://doi.org/10.1002/adfm.201900684.

29. G. Albano, G. Pescitelli, and L. D. Bari, "Chiroptical Properties in Thin Films of pi-Conjugated Systems," *Chemical Reviews* 120, no. 18 (2020): 10145–10243, https://doi.org/10.1021/acs.chemrev.0c00195.

30. J. Wade, J. N. Hilfiker, J. R. Brandt, et al., "Natural Optical Activity as the Origin of the Large Chiroptical Properties in Pi-Conjugated Polymer Thin Films," *Nature Communications* 11, no. 1 (2020): 6137, https://doi.org/10.1038/s41467-020-19951-y.

31. Y. Deng, M. Wang, Y. Zhuang, S. Liu, W. Huang, and Q. Zhao, "Circularly Polarized Luminescence From Organic Micro-/Nano-Structures," *Light: Science & Applications* 10, no. 1 (2021): 76, https://doi.org/10.1038/s41377-021-00516-7.

32. D. Giavazzi, M. F. Schumacher, L. Grisanti, et al., "A Marvel of Chiral Squaraine Aggregates: Chiroptical Spectra Beyond the Exciton Model," *Journal of Materials Chemistry C* 11, no. 24 (2023): 8307–8321, https://doi.org/10.1039/D2TC05555D.

33. M. Schulz, J. Zablocki, O. S. Abdullaeva, et al., "Giant Intrinsic Circular Dichroism of Prolinol-Derived Squaraine Thin Films," *Nature Communications* 9, no. 1 (2018): 2413, https://doi.org/10.1038/s41467-018-04811-7.

34. T. Quenzel, D. Timmer, M. Gittinger, et al., "Plasmon-Enhanced Exciton Delocalization in Squaraine-Type Molecular Aggregates," *ACS Nano* 16, no. 3 (2022): 4693–4704, https://doi.org/10.1021/acsnano.1c11398.

35. M. S. Vezie, S. Few, I. Meager, et al., "Exploring the Origin of High Optical Absorption in Conjugated Polymers," *Nature Materials* 15, no. 7 (2016): 746–753, https://doi.org/10.1038/nmat4645.

36. R. K. Hylton, G. J. Tizzard, T. L. Threlfall, et al., "Are the Crystal Structures of Enantiopure and Racemic Mandelic Acids Determined by Kinetics or Thermodynamics?," *Journal of the American Chemical Society* 137, no. 34 (2015): 11095–11104, https://doi.org/10.1021/jacs.5b05938.

37. T. J. Wiegand, J. S. Sandoval, J. A. Cody, D. W. McCamant, and C. J. Collison, "Directional Exciton Diffusion, Measured by Subpicosecond Transient Absorption as an Explanation for Squaraine Solar Cell Performance," *Journal of Physical Chemistry C* 128, no. 11 (2024): 4616–4630, https://doi.org/10.1021/acs.jpcc.3c06361.

38. C. Zheng, M. F. Mark, T. Wiegand, et al., "Measurement and Theoretical Interpretation of Exciton Diffusion as a Function of Intermolecular Separation for Squaraines Targeted for Bulk Heterojunction Solar Cells," *Journal of Physical Chemistry C* 124, no. 7 (2020): 4032–4043, https://doi.org/10.1021/acs.jpcc.9b11816.

39. L. D. Bakalis and J. Knoester, "Pump-Probe Spectroscopy and the Exciton Delocalization Length in Molecular Aggregates," *Journal of Physical Chemistry B* 103, no. 31 (1999): 6620–6628, https://doi.org/10.1021/jp990354g.

40. D. Timmer, F. Zheng, M. Gittinger, et al., "Charge Delocalization and Vibronic Couplings in Quadrupolar Squaraine Dyes," *Journal of the American Chemical Society* 144, no. 41 (2022): 19150–19162, https://doi.org/10.1021/jacs.2c08682.

41. C. Ruckebusch, M. Sliwa, P. Pernot, A. de Juan, and R. Tauler, "Comprehensive Data Analysis of Femtosecond Transient Absorption Spectra: A review," *Journal of Photochemistry and Photobiology C: Photochemistry Reviews* 13, no. 1 (2012): 1–27, https://doi.org/10.1016/j.jphotochemrev.2011.10.002.

42. H. P. Pasanen, R. Khan, J. A. Odutola, and N. V. Tkachenko, "Transient Absorption Spectroscopy of Films: Impact of Refractive Index," *Journal of Physical Chemistry C* 128, no. 15 (2024): 6167–6179, https://doi.org/10.1021/acs.jpcc.4c00981.

43. A. Ashoka, R. R. Tamming, A. V. Girija, et al., "Extracting Quantitative Dielectric Properties From Pump-Probe Spectroscopy," *Nature Communications* 13, no. 1 (2022): 1437, https://doi.org/10.1038/s41467-022-29112-y.

44. P. Malý, J. Lüttig, P. A. Rose, et al., "Separating Single- From Multi-Particle Dynamics in Nonlinear Spectroscopy," *Nature* 616, no. 7956 (2023): 280–287, https://doi.org/10.1038/s41586-023-05846-7.

45. D. Fazzi, M. Barbatti, and W. Thiel, "Unveiling the Role of Hot Charge-Transfer States in Molecular Aggregates via Nonadiabatic Dynamics," *Journal of the American Chemical Society* 138, no. 13 (2016): 4502–4511, https://doi.org/10.1021/jacs.5b13210.

46. R. Binder, M. Polkehn, T. Ma, and I. Burghardt, "Ultrafast Exciton Migration in an HJ-Aggregate: Potential Surfaces and Quantum Dynamics," *Chemical Physics* 482 (2017): 16–26, https://doi.org/10.1016/j.chemphys.2016.09.037.

47. A. Schubert, V. Settels, W. Liu, et al., "Ultrafast Exciton Self-Trapping Upon Geometry Deformation in Perylene-Based Molecular Aggregates," *Journal of Physical Chemistry Letters* 4, no. 5 (2013): 792–796, https://doi.org/10.1021/jz4000752.

48. B. Manna, R. Ghosh, and D. K. Palit, "Exciton Dynamics in Anthracene Nanoaggregates," *Journal of Physical Chemistry C* 119, no. 19 (2015): 10641–10652, https://doi.org/10.1021/acs.jpcc.5b00469.

49. X. Fan, A. Wei, T. Klamroth, Y. Zhang, K. Gao, and L. Wang, "Ultrafast Multiexciton Dynamics in Molecular Systems: Inclusion of Exciton-Exciton Annihilation," *Physical Review B* 107, no. 13 (2023): 134301, https://doi.org/10.1103/PhysRevB.107.134301.

50. A. De Sio, E. Sommer, X. T. Nguyen, et al., "Intermolecular Conical Intersections in Molecular Aggregates," *Nature Nanotechnology* 16, no. 1 (2021): 63–68, https://doi.org/10.1038/s41565-020-00791-2.

51. A. J. Musser, M. Liebel, C. Schnedermann, et al., "Evidence for Conical Intersection Dynamics Mediating Ultrafast Singlet Exciton Fission," *Nature Physics* 11, no. 4 (2015): 352–357, https://doi.org/10.1038/nphys3241.

52. M. J. Paterson, L. Blancafort, S. Wilsey, and M. A. Robb, "Photoinduced Electron Transfer in Squaraine Dyes: Sensitization of Large Band Gap Semiconductors," *Journal of Physical Chemistry A* 106, no. 47 (2002): 11431–11439, https://doi.org/10.1021/jp026418w.

53. G. de Miguel, M. Marchena, M. Zitnan, S. S. Pandey, S. Hayase, and A. Douhal, "Femto to Millisecond Observations of Indole-Based Squaraine Molecules Photodynamics in Solution," *Physical Chemistry Chemical Physics* 14, no. 5 (2012): 1796–1805, https://doi.org/10.1039/C1CP22864A.

54. B. G. Levine, M. P. Esch, B. S. Fales, D. T. Hardwick, W. T. Peng, and Y. Shu, "Conical Intersections at the Nanoscale: Molecular Ideas for Materials," *Annual Review of Physical Chemistry* 70 (2019): 21–43, https://doi.org/10.1146/annurev-physchem-042018-052425.

55. D. Polli, P. Altoé, O. Weingart, et al., "Conical Intersection Dynamics of the Primary Photoisomerization Event in Vision," *Nature* 467, no. 7314 (2010): 440–443, https://doi.org/10.1038/nature09346.

56. Y. Wu and J. E. Subotnik, "Electronic Spin Separation Induced by Nuclear Motion Near Conical Intersections," *Nature Communications* 12, no. 1 (2021): 700, https://doi.org/10.1038/s41467-020-20831-8.

57. M. S. Schuurman and A. Stolow, "Dynamics at Conical Intersections," *Annual Review of Physical Chemistry* 69 (2018): 427–450, https://doi.org/10.1146/annurev-physchem-052516-050721.

58. V. Settels, A. Schubert, M. Tafipolski, et al., "Identification of Ultrafast Relaxation Processes As a Major Reason for Inefficient Exciton Diffusion in Perylene-Based Organic Semiconductors," *Journal of the American Chemical Society* 136, no. 26 (2014): 9327–9337, https://doi.org/10.1021/ja413115h.

59. H. G. Duan, P. Nalbach, R. J. D. Miller, and M. Thorwart, "Ultrafast Energy Transfer in Excitonically Coupled Molecules Induced by a

26924560, 2025, 3, Downloaded from https://onlinelibrary.wiley.com/doi/10.1002/agt2.698 by Bibl. der Universitat zu Koln, Wiley Online Library on [12/11/2026]. See the Terms and Conditions (https://onlinelibrary.wiley.com/terms-and-conditions) on Wiley Online Library for rules of use; OA articles are governed by the applicable Creative Commons License

Nonlocal Peierls Phonon," *Journal of Physical Chemistry Letters* 10, no. 6 (2019): 1206–1211, https://doi.org/10.1021/acs.jpclett.9b00242.

60. O. Arteaga and R. Ossikovski, "Complete Mueller Matrix From a Partial Polarimetry Experiment: The 12-Element Case," *Journal of the Optical Society of America A* 36, no. 3 (2019): 416–427, https://doi.org/10.1364/JOSAA.36.000416.

61. E. Jung, K. Budzinauskas, S. Öz, et al., "Femto- to Microsecond Dynamics of Excited Electrons in a Quadruple Cation Perovskite," *ACS Energy Letters* 5, no. 3 (2020): 785–792, https://doi.org/10.1021/acsenergylett.9b02684.

Supporting Information

Additional supporting information can be found online in the Supporting Information section.

26924560, 2025, 3, Downloaded from https://onlinelibrary.wiley.com/doi/10.1002/agt2.698 by Bibl. der Universitat zu Koln, Wiley Online Library on [12/11/2026]. See the Terms and Conditions (https://onlinelibrary.wiley.com/terms-and-conditions) on Wiley Online Library for rules of use; OA articles are governed by the applicable Creative Commons License